# Supporting Information

## Piotrowski et al. 10.1073/pnas.1410400112

### SI Methods

**Compounds, Initial Screening, and Growth.** The diferulate compounds tested were synthesized as described by Lu et al. (1) and resuspended in DMSO. Caspofungin, nikkomycin Z, and MMS were purchased from Sigma-Aldrich. Echinocandin B was a gift from O. Kondo (Chugai Pharmaceuticals, Tokyo, Japan). Micafungin was provided by Astellas Pharma. Diferulates were initially screened at a concentration of 1 mg/mL to determine bioactivity. Cells of *Saccharomyces cerevisiae* (MATα *pdr1*Δ::*natMX pdr3*Δ::*KI.URA3 snq2*Δ::*KI.LEU2 can1*Δ::*STE2pr-Sp_his5 lyp1*Δ *his3*Δ1 *leu2*Δ0 *ura3*Δ0 *met15*Δ0), referred to as the control strain, were grown in 200-μL cultures at 30 °C in YPD with a drug or DMSO control. Plates were read on a TECAN M1000 over a 48-h growth period. The specific growth rate was calculated using GCAT analysis software (https://gcat3-pub.glbrc.org/) (2). When presented, $IC_{50}$ values for growth rate inhibition were calculated from triplicate eight-point dose curves and SigmaPlot 12.0. When presented, error bars are means ± SEs of at least three replicates.

**Determining the Most Sensitive Pathway Through Chemical Genomics.** A complex/pathway score based on chemical genomic data to identify protein complexes or pathways was developed based on which members showed significant deviation in their chemical genetic interactions in the presence of a compound. For each complex, the chemical genetic interaction score of the genes in the complex with the compound was summed. To determine significance, the expectations for such a sum for random sets of genes of equal size were calculated. The random sets of equal size were expected to have means equal to the background mean and SDs equal to the background SD/sqrt($n$). With this information, a $z$ score (number of SDs from the expected mean) for each complex or pathway can be computed:

$$\text{Pathway } z \text{ score} = (\Sigma/n - \mu)/(\sigma \times \text{sqrt}(n)),$$

where Σ = sum of the chemical genetic interaction scores of genes in the complex, μ = mean of the chemical genetic interaction scores of the compounds with all genes studies, σ = SD of chemical genetic interaction scores of the compounds with all genes in the study, and $n$ = size of the complex.

**Isolation, Sequencing, and Evaluation of Drug-Resistant Mutants.** Agar containing 500 μg/mL poacic acid was inoculated with ∼1 million cells of yeast (control strain). After 1 wk, two colonies were found growing on the agar. Single-colony isolates were obtained and found to be resistant to poacic acid. For whole-genome sequencing, single-colony isolates of poacic acid-resistant mutant, the caspofungin-resistant mutant, and the control strain (WT) were grown in triplicate 200-μL cultures and pooled for genomic DNA extraction (Epicentre MasterPure Yeast Kit; MPY80200). The genomic DNA was prepared for Illumina whole-genome sequencing using the Illumina TruSeqKkit (FC-121-3001) and sequenced by 150-bp paired-end reads on the MiSeq platform.

To determine mutations in the drug-resistant mutants, read quality analysis was performed using FastQC (www.bioinformatics.babraham.ac.uk/projects/fastqc/). Short reads were examined for quality and trimmed at the 3′ end when average base quality in a 3-nt window fell below Q30. Short reads were mapped to the standard *S. cerevisiae* reference genome, strain S288c (obtained from the National Center for Biotechnology Information RefSeq repository), using Burrows-Wheeler Alignment (BWA version 0.6.2) (3) using the default parameters, with the exception of the fraction of missing alignments threshold, which was set at 0.08 (–n in bwa aln). SNP and indel detection were performed with the Genome Analysis Toolkit (GATK version 1.4) (4) following their best practice variant-calling workflow (https://www.broadinstitute.org/gatk/). Duplicate reads were marked followed by base quality recalibration using a single nucleotide polymorphism database designed for *S. cerevisiae*. To minimize false-positive variant calls, stringent parameters were used: namely, the minimum base quality required to consider a base for calling was 30, and the minimum phred-scaled confidence threshold for genotype calling was 50 (–mbq and –scc in the UnifiedGenotyper tool). Custom Perl scripts were used to further filter calls on the basis of read depth, mapping quality, and strand bias. This analysis revealed an SNP in the gene *SUR1* (glutamate > stop codon) in the poacic acid-resistant mutant.

**Cell Leakage Assays.** A FungaLight Cell Viability Assay (L34952; Invitrogen) using a Guava Flow Cytometer (Millipore) was used to determine if poacic acid caused membrane damage. The population of stained cells (damaged integrity) vs. nonstained cells can be determined by flow cytometry. Caspofungin (50 ng/mL) was included as a positive control. MMS and DMSO were included as a noncell wall-targeting control and a solvent control, respectively. To test the effects of the compounds on both active and arrested cells, log-phase cultures were washed with 1× PBS and resuspended to an $OD_{0.5}$ in either YPD medium or YP (no carbon source) in the presence of the drugs ($n$ = 3) for 4 h at 30 °C. The cells were then stained and immediately read by flow cytometry. One-way ANOVA and Tukey's test were used to calculate the difference between drug treatments among cells with arrested growth.

**Synergy Screening.** To test for synergy, a 6 × 6-dose matrix was initially used to identify potentially synergistic dose combinations, and these points were then confirmed in triplicate. Cultures (200 μL) were grown with combinations of poacic acid (125 μg/mL), caspofungin (12.5 ng/mL), and fluconazole (3.8 μg/mL), and the ODs of relevant single-agent and solvent controls were measured after 24 h. Synergy was determined by comparing actual OD in the presence of compound combinations with an expected value calculated using the multiplicative hypothesis. This method assumes that, in the absence of an interaction, each compound would decrease the OD of the cell culture by the same fraction in the presence of the other compound as it does when applied alone (that is, $E = A \times B/C$, where $E$ is the expected OD, $A$ is OD when compound A is applied alone, $B$ is OD when compound B is applied alone, and $C$ is OD of the control culture (DMSO). In the presence of synergy, the actual OD value is lower than the expected OD. A paired $t$ test was used to confirm statistical significance of this difference in three replicates of the experiment.

**Staining of Cells with Poacic Acid.** Log-phase yeast cells (*his3*Δ) were harvested by centrifugation, washed two times with PBS, sonicated mildly, and then, incubated with 0.25% (wt/vol) poacic acid for 5 min. A small aliquot of the cells was mounted on a glass slide and observed under an Axioimager M1 Fluorescence Microscope (Carl Zeiss) using the XF09 Filter Set (Opto Science; excitation wavelength, 340–390 nm; emission wavelength, 517.5–552.5 nm).

**Mannoprotein and Glucan Staining.** β-1,3-Glucan was stained with aniline blue (016-21302; Wako Chemicals) as described previously

(5) with slight modification. Briefly, log-phase yeast cells (*his3*Δ) were cultured in YPD with poacic acid (125 μg/mL) at 25 °C. Then, cells were collected at 0, 2, 4, and 6 h after treatment and stained with aniline blue without fixation as described previously (6). Cells mounted on a glass slide were exposed to UV for 30 s to bleach out poacic acid fluorescence before acquiring images. Staining of chitin or mannoproteins with calcofluor white (F3543; Sigma-Aldrich) or Alexa594-ConA (C11253; Life Technologies), respectively, was performed as described previously (6). For cell-free glucan staining, yeast glucan (G0331; Tokyo Chemical Industry) was suspended to 0.125% (wt/vol) poacic acid and observed under a fluorescent microscope using a regular DAPI filter set (Carl Zeiss).

**Determination of Ferulate and Diferulates by Reverse-Phase HPLC–High-Resolution/Accurate MS in Hydrolysates.** Ammonia fiber expansion treated corn stover hydrolysates samples were diluted 1:10, and 20-μL samples were analyzed by reverse-phase (C18) HPLC–high-resolution/accurate MS. Peak areas of peaks matching in retention time and accurate mass ± 10 ppm of authentic reference standards were used to calculate concentrations by comparison with an external standard curve.


1. Lu F, Wei L, Azarpira A, Ralph J (2012) Rapid syntheses of dehydrodiferulates via biomimetic radical coupling reactions of ethyl ferulate. *J Agric Food Chem* 60(34):8272–8277.
2. Sato TK, et al. (2014) Harnessing genetic diversity in Saccharomyces cerevisiae for improved fermentation of xylose in hydrolysates of alkaline hydrogen peroxide pretreated biomass. *Appl Environ Microbiol* 80(2):540–554.
3. Li H, Durbin R (2009) Fast and accurate short read alignment with Burrows-Wheeler transform. *Bioinformatics* 25(14):1754–1760.
4. DePristo MA, et al. (2011) A framework for variation discovery and genotyping using next-generation DNA sequencing data. *Nat Genet* 43(5):491–498.
5. Watanabe D, Abe M, Ohya Y (2001) Yeast Lrg1p acts as a specialized RhoGAP regulating 1,3-β-glucan synthesis. *Yeast* 18(10):943–951.
6. Okada H, Ohya Y (2015) *Cold Spring Harbor Protocols* (Cold Spring Harbor Lab Press, Plainview, NY).


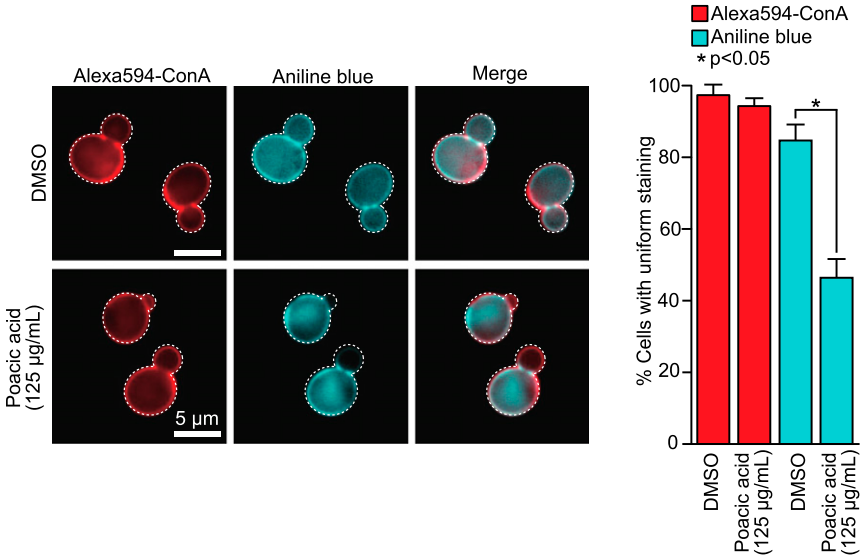


**Fig. S1.** Poacic acid treatment reduces glucan staining with aniline blue but has no effect on mannoprotein straining. The control strain yeast cells (*his3*Δ) were grown in YPD at 25 °C until early log phase, transferred to fresh YPD medium containing poacic acid (125 μg/mL) or DMSO [0.125% (vol/vol)] as a solvent control, and cultured for 6 h. The cells were collected, and the cell wall components mannoproteins were stained with Alexa594-conjugated Con A followed by β-1,3-glucan staining with aniline blue. The cells were observed under a fluorescent microscope, and over 150 budding cells were counted according to the staining signal from three independent experiments. A Student's *t* test was used to determine significant differences (mean ± SE; $n = 3$).

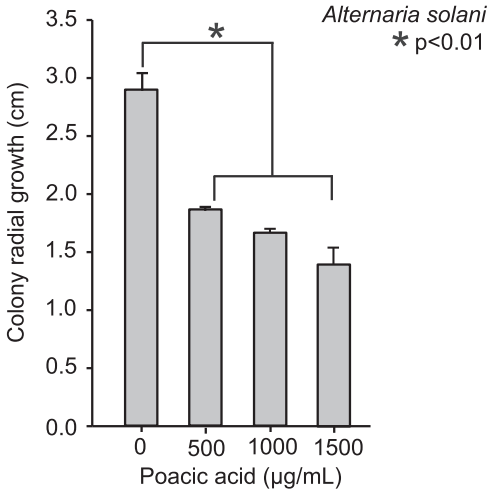


**Fig. S2.** Poacic acid significantly inhibits colony growth of *Alternaria solani*. Colony growth on plates of *A. solani* (field isolate) was significantly ($P < 0.01$) inhibited by poacic acid in a dose-dependent manner. One-way ANOVA and Tukey's test were used to evaluate the difference between drug treatments among treatments (mean ± SE; $n = 3$).

**Table S1. Nomenclature, molecular weight, and IUPAC names of diferulate derivatives tested**

| Name | Description | Molecular weight | IUPAC |
|---|---|---|---|
| 8–8-C | 8–8-coupled cyclic diferulic acid | 386 | *trans*-7-Hydroxy-1-(4-hydroxy-3-methoxyphenyl)-6-methoxy-1,2-dihydronaphthalene-2,3-dicarboxylic acid |
| 4–O–5 | 4–O–5-coupled diferulic acid | 386 | (*E*)-3-{4- [(*E*)-2-Carboxyvinyl]-2-methoxyphenoxy}-4-hydroxy-5-methoxycinnamic acid |
| 8–5-C | 8–5-coupled cyclic diferulic acid | 386 | *trans*-5-[(*E*)-2-carboxyvinyl]-2- (4-hydroxy-3-methoxyphenyl)-7-methoxy-2,3-dihydrobenzo-furan-3-carboxylic acid |
| 8–8-O | 8–8-coupled opened diferulic acid | 386 | 4,4′-Dihydroxy-5,5′-dimethoxy-8,8′-bicinnamic acid |
| 8–8-THF | 8–8-coupled tetrahydrofuran diferulic acid | 404 | 2,5-bis-(4-Hydroxy-3-methoxyphenyl)-tetrahydrofuran-3,4-dicarboxylic acid |
| 8–O–4 | 8–O–4-coupled diferulic acid | 386 | (*Z*)-8-{4-[(*E*)-2-Carboxyvinyl]-2-methoxyphenoxy}-4-hydroxy-3-methoxy-cinnamic acid |
| 5–5 | 5–5-coupled diferulic acid | 386 | (*E,E*)-4,4′-Dihydroxy-5,5′-dimethoxy-3,3′-bicinnamic acid |
| 8–5-O | 8–5-coupled opened diferulic acid | 386 | (*E,E*)-4,4′-dihydroxy-3,5′-dimethoxy-8,3′-bicinnamic acid |
| 8–5-DC (poacic acid) | 8–5-coupled decarboxy diferulic acid | 342 | (*E*)-4-Hydroxy-3-{2-[(E)-4-hydroxy-3-methoxystyryl]}-5-methoxycinnamic acid |

IUPAC, International Union of Pure and Applied Chemistry.

**Table S2. Top 10 sensitive and resistant deletion mutants among the poacic acid-treated deletion collection**

| Gene | *z* Score | *P* adjusted | Description |
|---|---|---|---|
| Sensitive mutants | | | |
| *BCK1* | −12.91 | 2.58E-28 | MAPKKK acting in the PKC signaling pathway; the kinase C signaling pathway controls cell integrity; on activation by Pkc1p phosphorylates downstream kinases Mkk1p and Mkk2p |
| *CWH43* | −10.99 | 7.98E-7 | Putative sensor/transporter protein involved in cell wall biogenesis; contains 14–16 transmembrane segments and several putative glycosylation and phosphorylation sites; null mutation is synthetically lethal with pkc1 deletion |
| *RGD1* | −10.16 | 1.21E-7 | GTPase-activating protein (RhoGAP) for Rho3p and Rho4p; possibly involved in control of actin cytoskeleton organization |
| *ROM2* | −9.47 | 8.88E-8 | GDP/GTP exchange factor (GEF) for Rho1p and Rho2p; mutations are synthetically lethal with mutations in rom1, which also encodes a GEF; Rom2p localization to the bud surface is dependent on Ack1p; *ROM2* has a paralog, *ROM1*, that arose from the whole-genome duplication |
| *FYV8* | −9.11 | 1.11E-14 | Protein of unknown function; required for survival on exposure to K1 killer toxin |
| *ACK1* | −9.09 | 1.39E-5 | Protein that functions in the cell wall integrity pathway; functions upstream of Pkc1p; GFP-fusion protein expression is induced in response to the DNA-damaging agent MMS; nontagged Ack1p is detected in purified mitochondria |
| *ALG6* | −8.30 | 1.82E-11 | α1,3-Glucosyltransferase; involved in transfer of oligosaccharides from dolichyl pyrophosphate to asparagine residues of proteins during N-linked protein glycosylation; mutations in human ortholog are associated with disease |
| *EMC4* | −7.92 | 1.90E-3 | Member of conserved ER transmembrane complex; required for efficient folding of proteins in the ER; null mutant displays induction of the unfolded protein response |
| *SNG1* | −7.91 | 8.96E-13 | Protein involved in resistance to nitrosoguanidine and 6-azauracil; expression is regulated by transcription factors involved in multidrug resistance; SNG1 has a paralog, YJR015W, that arose from the whole-genome duplication |
| *ERG2* | −7.80 | 4.76E-3 | C-8 sterol isomerase; catalyzes the isomerization of the delta-8 double bond to the delta-7 position at an intermediate step in ergosterol biosynthesis |
| Resistant mutants | | | |
| *CSG2* | 5.89 | 1.57E-3 | Endoplasmic reticulum membrane protein; required for mannosylation of inositolphosphorylceramide and growth at high calcium concentrations; protein abundance increases in response to DNA replication stress |
| *LCL1* | 5.79 | 4.51E-3 | Putative protein of unknown function; deletion mutant is fluconazole resistant and has long chronological lifespan |
| *DFG5* | 5.51 | 1.34E-2 | Putative mannosidase; essential GPI-anchored membrane protein required for cell wall biogenesis in bud formation, involved in filamentous growth, homologous to Dcw1p |
| *NBP2* | 5.43 | 1.57E-3 | Protein involved in the high osmolarity glycerol (HOG) pathway; negatively regulates Hog1p by recruitment of phosphatase Ptc1p and the Pbs2p-Hog1p complex; interacts with Bck1p and down-regulates the cell wall integrity pathway; found in the nucleus and cytoplasm, contains an SH3 domain and a Ptc1p binding domain |
| *RTS1* | 5.39 | 6.26E-3 | B-type regulatory subunit of protein phosphatase 2A (PP2A); Rts1p and Cdc55p are alternative regulatory subunits for PP2A catalytic subunits, Pph21p and Pph22p; PP2A-Rts1p protects cohesin when recruited by Sgo1p to the pericentromere; highly enriched at centromeres in the absence of Cdc55p; required for maintenance of septin ring organization during cytokinesis, ring disassembly in G1, and dephosphorylation of septin, Shs1p; homolog of the mammalian B subunit of PP2A |
| *NUP170* | 5.33 | 2.79E-6 | Subunit of the inner ring of the nuclear pore complex (NPC); contributes to NPC assembly and nucleocytoplasmic transport; both Nup170p and Nup157p are similar to human Nup155p; *NUP170* has a paralog, *NUP157*, that arose from the whole-genome duplication |
| *DSF2* | 5.32 | 6.68E-5 | Deletion suppressor of mpt5 mutation; relocalizes from bud neck to cytoplasm on DNA replication stress |
| *SUR1* | 5.21 | 5.34E-3 | Mannosylinositol phosphorylceramide synthase catalytic subunit; forms a complex with regulatory subunit Csg2p; function in sphingolipid biosynthesis is overlapping with that of Csh1p; *SUR1* has a paralog, *CSH1*, that arose from the whole-genome duplication |
| *PIB2* | 4.96 | 2.79E-6 | Protein of unknown function; contains FYVE domain; similar to Fab1 and Vps27 |
| *RPL21B* | 4.81 | 1.11E-5 | Ribosomal 60S subunit protein L21B; homologous to mammalian ribosomal protein L21, no bacterial homolog; *RPL21B* has a paralog, *RPL21A*, that arose from the whole-genome duplication |

**Table S3. Deletion mutants with significant morphological correlations with poacic acid-treated cells**

| Gene | *R* value | *P* with Bonferroni correction | Description |
|---|---|---|---|
| *COG1* | 0.61 | 1.52E-8 | Essential component of the conserved oligomeric Golgi complex (Cog1p–Cog8p), a cytosolic tethering complex that functions in protein trafficking to mediate fusion of transport vesicles to Golgi compartments |
| *NPY1* | 0.61 | 2.08E-8 | NADH diphosphatase (pyrophosphatase) hydrolyzes the pyrophosphate linkage in NADH and related nucleotides; localizes to peroxisomes; nudix hydrolase family member |
| *SUR4* | 0.61 | 2.25E-8 | Elongase involved in fatty acid and sphingolipid biosynthesis; synthesizes very long-chain 20–26-carbon fatty acids from C18-CoA primers; involved in regulation of sphingolipid biosynthesis |
| *OST4* | 0.61 | 3.31E-8 | Subunit of the oligosaccharyltransferase complex of the endoplasmic reticulum (ER) lumen, which catalyzes protein asparagine-linked glycosylation; type I membrane protein required for incorporation of Ost3p or Ost6p into the OST complex |
| *OST3* | 0.61 | 3.75E-8 | γ-Subunit of the oligosaccharyltransferase complex of the ER lumen, which catalyzes asparagine-linked glycosylation of newly synthesized proteins; Ost3p is important for *N*-glycosylation of a subset of proteins |
| *YLR111W* | 0.60 | 4.20E-8 | Dubious ORF unlikely to encode a protein based on available experimental and comparative sequence data |
| *YAL058C-A* | 0.60 | 4.24E-8 | Dubious ORF unlikely to encode a protein based on available experimental and comparative sequence data |
| *SNC2* | 0.60 | 5.53E-8 | Vesicle membrane receptor protein (v-SNARE); involved in the fusion between Golgi-derived secretory vesicles with the plasma membrane; member of the synaptobrevin/VAMP family of R-type v-SNARE proteins; *SNC2* has a paralog, *SNC1*, that arose from the whole-genome duplication |
| *FKS1* | 0.59 | 1.01E-7 | Catalytic subunit of 1,3-β-D-glucan synthase; functionally redundant with alternate catalytic subunit Gsc2p; binds to regulatory subunit Rho1p; involved in cell wall synthesis and maintenance; localizes to sites of cell wall remodeling; *FKS1* has a paralog, *GSC2*, that arose from the whole-genome duplication |
| *BNI1* | 0.59 | 2.39E-7 | Formin, nucleates the formation of linear actin filaments, involved in cell processes, such as budding and mitotic spindle orientation, which require the formation of polarized actin cables, functionally redundant with *BNR1* |
| *SWA2* | 0.59 | 2.41E-7 | Auxilin-like protein involved in vesicular transport; clathrin-binding protein required for uncoating of clathrin-coated vesicles |
| *GAS1* | 0.58 | 5.56E-7 | β-1,3-Glucanosyltransferase, required for cell wall assembly and also has a role in transcriptional silencing; localizes to the cell surface through a GPI anchor; also found at the nuclear periphery |
| *PER1* | 0.57 | 1.14E-6 | Protein of the endoplasmic reticulum, required for GPI-phospholipase A2 activity that remodels the GPI anchor as a prerequisite for association of GPI-anchored proteins with lipid rafts; functionally complemented by human ortholog PERLD1 |
| *OCH1* | 0.57 | 1.34E-6 | Mannosyltransferase of the *cis*-Golgi apparatus, initiates the polymannose outer-chain elongation of N-linked oligosaccharides of glycoproteins |
| *MNN11* | 0.55 | 6.42E-6 | Subunit of a Golgi mannosyltransferase complex that also contains Anp1p, Mnn9p, Mnn10p, and Hoc1p and mediates elongation of the polysaccharide mannan backbone; has homology to Mnn10p |
| *CAX4* | 0.55 | 7.14E-6 | Dolichyl pyrophosphate (Dol-P-P) phosphatase with a luminally oriented active site in the ER cleaves the anhydride linkage in Dol-P-P, required for Dol-P-P–linked oligosaccharide intermediate synthesis and protein *N*-glycosylation |
| *MON2* | 0.54 | 1.13E-5 | Peripheral membrane protein with a role in endocytosis and vacuole integrity, interacts with Arl1p and localizes to the endosome; member of the Sec7p family of proteins |
| *KRE1* | 0.53 | 2.30E-5 | Cell wall glycoprotein involved in β-glucan assembly; serves as a K1 killer toxin membrane receptor |
| *DFG5* | 0.52 | 4.40E-5 | Putative mannosidase, essential GPI-anchored membrane protein required for cell wall biogenesis in bud formation, involved in filamentous growth, homologous to Dcw1p |
| *GUP1* | 0.51 | 8.67E-5 | Plasma membrane protein involved in remodeling GPI anchors; member of the MBOAT family of putative membrane-bound O-acyltransferases; proposed to be involved in glycerol transport; *GUP1* has a paralog, *GUP2*, that arose from the whole-genome duplication |
| *TPM1* | 0.51 | 1.02E-4 | Major isoform of tropomyosin; binds to and stabilizes actin cables and filaments, which direct polarized cell growth and the distribution of several organelles; acetylated by the NatB complex and acetylated form binds actin most efficiently; *TPM1* has a paralog, *TPM2*, that arose from the whole-genome duplication |
| *YOL013W-A* | 0.51 | 1.09E-04 | Putative protein of unknown function; identified by SAGE |
| *RHO4* | 0.51 | 1.10E-4 | Nonessential small GTPase; member of the Rho/Rac subfamily of Ras-like proteins; likely to be involved in the establishment of cell polarity; has long N-terminal extension that plays an important role in Rho4p function and is shared with Rho4 homologs in other yeasts and filamentous fungi |
| *ALG8* | 0.48 | 7.48E-4 | Glucosyl transferase, involved in N-linked glycosylation; adds glucose to the dolichol-linked oligosaccharide precursor before transfer to protein during lipid-linked oligosaccharide biosynthesis; similar to Alg6p |
| *VPS52* | 0.48 | 9.14E-4 | Component of the Golgi-associated retrograde protein (GARP) complex, Vps51p-Vps52p-Vps53p-Vps54p, which is required for the recycling of proteins from endosomes to the late Golgi; involved in localization of actin and chitin |

**Table S3. Cont.**

| Gene | *R* value | *P* with Bonferroni correction | Description |
|---|---|---|---|
| *GDT1* | 0.47 | 1.26E-3 | Protein of unknown function involved in calcium homeostasis; localizes to the *cis*- and medial-Golgi apparatus; GFP-fusion protein localizes to the vacuole; TMEM165, a human gene that causes congenital disorders of glycosylation is orthologous and functionally complements the null allele; expression pattern and physical interactions suggest a possible role in ribosome biogenesis; expression reduced in a gcr1 null mutant |
| *UME1* | 0.47 | 1.42E-3 | Negative regulator of meiosis; required for repression of a subset of meiotic genes during vegetative growth, binding of histone deacetylase Rpd3p required for activity, contains an NEE box and a WD repeat motif; homologous with Wtm1p; *UME1* has a paralog, *WTM2*, that arose from the whole-genome duplication |
| *CLC1* | 0.46 | 2.19E-3 | Clathrin light chain; subunit of the major coat protein involved in intracellular protein transport and endocytosis; thought to regulate clathrin function; two Clathrin heavy chains (CHC1) form the clathrin triskelion structural component; *YGR167W* |
| *MMS2* | 0.46 | 2.87E-3 | Subunit of an E3 ubiquitin ligase complex involved in replication repair; stabilizes protein components of the replication fork, such as the fork-pausing complex and leading strand polymerase, preventing fork collapse and promoting efficient recovery during replication stress; required for accurate meiotic chromosome segregation |
| *IMP2* | 0.46 | 2.91E-3 | Transcriptional activator involved in maintenance of ion homeostasis and protection against DNA damage caused by bleomycin and other oxidants, contains a C-terminal leucine-rich repeat |
| *PEP5* | 0.46 | 3.17E-3 | Histone E3 ligase, component of CORVET tethering complex; peripheral vacuolar membrane protein required for protein trafficking and vacuole biogenesis; interacts with Pep7p; involved in ubiquitylation and degradation of excess histones |
| *YPL184C* | 0.46 | 3.43E-3 | RNA-binding protein that may be involved in translational regulation; binds specific categories of mRNAs, including those that contain upstream ORFs and internal ribosome entry sites; interacts genetically with chromatin remodelers and splicing factors, linking chromatin state, splicing and as a result, mRNA maturation |
| *PEP3* | 0.46 | 3.63E-3 | Component of CORVET tethering complex; vacuolar peripheral membrane protein that promotes vesicular docking/fusion reactions in conjunction with SNARE proteins, required for vacuolar biogenesis |
| *CAP1* | 0.45 | 3.76E-3 | α-Subunit of the capping protein heterodimer (Cap1p and Cap2p); capping protein binds to the barbed ends of actin filaments, preventing additional polymerization; localized predominantly to cortical actin patches; protein increases in abundance and relocalizes from bud neck to plasma membrane on DNA replication stress |
| *YFR016C* | 0.45 | 3.78E-3 | Putative protein of unknown function; GFP-fusion protein localizes to the cytoplasm and bud; interacts with Spa2p; YFL016C is not an essential gene |
| *PEA2* | 0.45 | 3.82E-3 | Coiled-coil polarisome protein required for polarized morphogenesis, cell fusion, and low-affinity $Ca^{2+}$ influx; forms polarisome complex with Bni1p, Bud6p, and Spa2p; localizes to sites of polarized growth |
| *BUD6* | 0.45 | 3.85E-3 | Actin- and formin-interacting protein; participates in actin cable assembly and organization as a nucleation-promoting factor for formins Bni1p and Bnr1p; involved in polarized cell growth; isolated as bipolar budding mutant; potential Cdc28p substrate |
| *VPS16* | 0.45 | 4.54E-3 | Subunit of the vacuole fusion and protein-sorting HOPS complex and the CORVET tethering complex; part of the class C Vps complex essential for membrane docking and fusion at Golgi-to-endosome and endosome-to-vacuole protein transport stages |
| *POC4* | 0.45 | 5.86E-3 | Component of a heterodimeric Poc4p-Irc25p chaperone involved in assembly of α-subunits into the 20S proteasome; may regulate formation of proteasome isoforms with alternative subunits under different conditions |
| *VPS33* | 0.45 | 6.49E-3 | ATP-binding protein that is a subunit of the HOPS complex and the CORVET tethering complex; essential for protein sorting, vesicle docking, and fusion at the vacuole |
| *OPT2* | 0.44 | 7.41E-3 | Oligopeptide transporter; member of the OPT family, with potential orthologs in *Schizosaccharomyces pombe* and *Candida albicans*; also plays a role in formation of mature vacuoles |
| *BNA1* | 0.44 | 8.62E-3 | 3-Hydroxyanthranilic acid dioxygenase, required for the de novo biosynthesis of NAD from tryptophan through kynurenine; expression regulated by Hst1p |
| *PPS1* | 0.44 | 8.99E-3 | Protein phosphatase with specificity for serine, threonine, and tyrosine residues; has a role in the DNA synthesis phase of the cell cycle |

**Table S4. Diferulates and ferulate concentration in ammonia fiber expansion-treated lignocellulosic hydrolysates (micromolar)**

| Pretreatment method | 8–8-O | 8–5-O | 8–8-THF | 5–5 | 8–O-4 | 8–5-C | Poacic acid | Ferulic acid |
|---|---|---|---|---|---|---|---|---|
| 6% AFEX-treated corn stover | 3.23 | <0.2 | 0.55 | 0.16 | 0.06 | 8.58 | 0.10 | 76.6 |

AFEX, ammonia fiber expansion.